Neuron
Article

Developmental Refinement of Vesicle Cycling at Schaffer Collateral Synapses

Tobias Rose,[1,3,*] Philipp Schoenenberger,[1,4] Karel Jezek,[2] and Thomas G. Oertner[1,5,*]
[1]Friedrich Miescher Institute for Biomedical Research, CH-4058 Basel, Switzerland
[2]Kavli Institute for Systems Neuroscience, CNC, NTNU, NO-7489 Trondheim, Norway
[3]Present address: Max Planck Institute of Neurobiology, D-82152 Martinsried, Germany
[4]Present address: IST Austria, Am Campus 1, A-3400 Klosterneuburg, Austria
[5]Present address: Institute for Synaptic Physiology, Center for Molecular Neurobiology Hamburg, D-20251 Hamburg, Germany
*Correspondence: trose@neuro.mpg.de (T.R.), thomas.oertner@zmnh.uni-hamburg.de (T.G.O.)
http://dx.doi.org/10.1016/j.neuron.2013.01.021

SUMMARY

At synapses formed between dissociated neurons, about half of all synaptic vesicles are refractory to evoked release, forming the so-called "resting pool." Here, we use optical measurements of vesicular pH to study developmental changes in pool partitioning and vesicle cycling in cultured hippocampal slices. Two-photon imaging of a genetically encoded two-color release sensor (ratio-sypHy) allowed us to perform calibrated measurements at individual Schaffer collateral boutons. Mature boutons released a large fraction of their vesicles during simulated place field activity, and vesicle retrieval rates were 7-fold higher compared to immature boutons. Saturating stimulation mobilized essentially all vesicles at mature synapses. Resting pool formation and a concomitant reduction in evoked release was induced by chronic depolarization but not by acute inhibition of the protein phosphatase calcineurin. We conclude that synapses in CA1 undergo a prominent refinement of vesicle use during early postnatal development that is not recapitulated in dissociated neuronal culture.

INTRODUCTION

Information transfer at chemical synapses relies on the availability of neurotransmitter-filled synaptic vesicles. Classically, these vesicles have been divided into two major pools (Rizzoli and Betz, 2005): the *recycling pool* encompasses all functional vesicles that can be mobilized upon action potential (AP) firing. The release-ready subset of these vesicles can be rapidly exocytosed and supports transmission during sporadic AP firing (Murthy et al., 2001; Schikorski and Stevens, 2001), whereas the remainder is recruited during sustained activity (Rizzoli and Betz, 2005). The second major pool—the so-called *resting pool*—contains all vesicles that are incapable of AP-evoked exocytosis. Pool definitions are operational; they depend on the measurement procedure. Glutamate released to the synaptic cleft, the most relevant parameter for synaptic function, cannot be compared reliably to the total vesicular glutamate reserve on a single synapse level. As a proxy, staining and destaining of vesicles by lipophilic FM dyes has been used. This method labels vesicles that collapse fully in the bouton membrane and remain exposed to the extracellular space for several seconds, until the membrane patch is recycled by clathrin-mediated endocytosis. If, however, some vesicles release transmitter without full collapse, they are not detectable by FM staining (Harata et al., 2006). To detect all vesicles that were in contact with the extracellular space, no matter how briefly, optical monitoring of vesicular pH is the method of choice. Genetically encoded pH indicators have been developed to measure the activity of hundreds of boutons simultaneously (Burrone et al., 2006; Fredj and Burrone, 2009; Granseth et al., 2006; Miesenböck et al., 1998; Sankaranarayanan and Ryan, 2000). In dissociated culture, pH-based methods consistently report a resting pool of about 50% (Fernandez-Alfonso and Ryan, 2008; Fredj and Burrone, 2009; Kim and Ryan, 2010; Li et al., 2005), whereas FM dye staining results in even larger values, up to 85% (Harata et al., 2001). The function of such a large nonreleasable pool is highly controversial. The resting pool could act as a reservoir of vesicles that can be mobilized after periods of synaptic disuse (Kim and Ryan, 2010), it might be accessed during NMDA-receptor-dependent presynaptic potentiation (Ratnayaka et al., 2012), it could support spontaneous vesicle release (Fredj and Burrone, 2009; Hua et al., 2011; Ramirez et al., 2012), or it could act as a local protein reservoir to buffer cytosolic proteins necessary for vesicle cycling (Denker et al., 2011b).

Synaptic properties change during development (Feldmeyer and Radnikow, 2009; Mozhayeva et al., 2002), a process that has been studied in detail at the calyx of Held, a giant synapse in the auditory brain stem (Borst and Soria van Hoeve, 2012). The immature calyx contains a large fraction of nonreleasable vesicles (de Lange et al., 2003), is unreliable, and shows pronounced short-term depression (Taschenberger and von Gersdorff, 2000). After hearing onset (P12–P14), it becomes very reliable and fast, driving the postsynaptic cell at high frequencies (Lorteije et al., 2009; Sonntag et al., 2011). At the

calyx, this altered short-term plasticity results from changes in synaptic release probability (P_r), vesicle pool sizes, and endocytic capacity (Renden and von Gersdorff, 2007; Taschenberger and von Gersdorff, 2000; Yamashita et al., 2010). Whether similar developmental changes also take place at much smaller cortical synapses is unclear. Experiments on acute hippocampal and neocortical slices suggested that short-term plasticity and P_r at small synapses develop similar to the calyx (Bolshakov and Siegelbaum, 1995; Feldmeyer and Radnikow, 2009; Reyes and Sakmann, 1999). In dissociated culture, on the other hand, endocytosis has been reported to be stable over time (Armbruster and Ryan, 2011), and the vesicle retrieval rate at saturating stimulation intensity (Sankaranarayanan and Ryan, 2000), that is, endocytic capacity, remains low compared to the mature calyx (Renden and von Gersdorff, 2007; Wu et al., 2009). The total number of vesicles increases during development (Mozhayeva et al., 2002), but it is unclear if partitioning into functional and nonfunctional pools is also developmentally regulated.

We set out to study the maturation of presynaptic function at Schaffer collateral (SC) synapses in slice cultures of rat hippocampus, a preparation that closely recapitulates postnatal development (De Simoni et al., 2003). To measure the fraction of released and recycling vesicles, we developed a dual-color release indicator (ratio-sypHy) for use in intact tissue. In immature slice cultures, after 5–7 days in vitro (DIV 5–7), a sizable fraction of vesicles could not be released. In 2–4 week cultures, however, essentially all vesicles were mobilized in response to either high-frequency AP trains or typical CA3 cell place field activity. The rate of vesicle retrieval increased about 7-fold during maturation. Chronic depolarization induced a sizable resting pool at mature SC boutons. Therefore, SC boutons are capable of reducing their output by removing vesicles from the recycling pool, but this homeostatic mechanism seems to be activated only during periods of pathologically high activity. We conclude that synapses in CA1 undergo a pronounced refinement of vesicle use and recycling during early postnatal development.

RESULTS

Characterization of Ratio-sypHy, a Dual-Color Indicator of Vesicle Release and Recycling

Our indicator is based on a fusion protein of the pH-sensitive GFP variant superecliptic pHluorin (Miesenböck et al., 1998) with the synaptic vesicle protein synaptophysin I (sypI), a combination known as sypHy (Granseth et al., 2006). To create a dual emission indicator suitable for ratiometric two-photon microscopy, we fused the extraluminal C terminus of sypHy with the dimeric red fluorescent protein tdimer2 (ratio-sypHy; Figure 1A). The C-terminal tdimer2-tag faces the cytoplasm, providing a red fluorescence signal proportional to the total amount of ratio-sypHy present at a synapse. Because of the fixed stoichiometry, the green-to-red fluorescence ratio of ratio-sypHy was independent of expression level and depth of the synapse in the tissue and could be compared across cells. To selectively transfect cells in hippocampal slice cultures, we aimed a Helios Gene Gun through an adjustable pinhole centered above CA3. A few days after transfection, we observed red fluorescent somata in CA3 and bright fluorescent puncta in CA1 (Figure 1B). Ratio-sypHy was effectively targeted to boutons, which were 23-fold brighter than the axonal shafts (Figure S1A available online). The probe showed a variable level of surface expression (median f_{surf} = 0.20, quartile coefficient of variation, QCV: 0.59, n = 922 boutons, 25 slices), which was correlated with its expression level (R^2 = 0.43, p = 0.0024, n = 19 cells; Figures S1C and S1D).

We stimulated individual ratio-sypHy expressing CA3 pyramidal cells and their axons by current injection in the whole-cell patch-clamp configuration. To release a sizable fraction of the total recycling pool at both high and low release probability (P_r) synapses, we evoked trains of 200 APs at 30 Hz by brief somatic current injections. This stimulation led to a robust increase in green but not in red fluorescence at individual boutons along single CA3 axons (Figure 1C). Differential bleaching of the red fluorescence by the imaging laser meant that only one ratiometric measurement per bouton could be performed. However, the fixed stoichiometry of green and red fluorescent proteins permitted sequential measurements to be calibrated on a separate set of boutons. To activate green fluorescence in *all* vesicles for calibration, we neutralized the pH of intracellular compartments by NH_4Cl or protonophores (see below) at the end of every experiment (Figures 1A and S1B). We corrected for photobleaching (Figures S1E and S1F), surface-stranded protein (see the Experimental Procedures), and calculated the released fraction (RF), that is, the number of released vesicles divided by the total number of vesicles present at the synapse (Figure 1D). This method of separating release measurements and calibration allowed us to quantify vesicle cycle parameters at a large number of consecutive boutons along individual axons irrespective of their depth in tissue. The large distance between optically recorded boutons and their somata (973 ± 109 μm, n = 12 cells) minimized potential artifacts from whole-cell dialysis.

Released Fractions at Individual Schaffer Collateral Boutons Are Heterogeneous and Not Correlated between Neighboring Boutons

The median RF at mature SC boutons (DIV 14–28) in response to 200 APs was 28.6% ± 3.3% (average of 12 cells). In all cells tested, RFs were variable between individual boutons (average QCV 0.30 ± 0.04; n = 12 cells, 5–90 boutons each) with a distribution skewed toward smaller RFs (Figures 1E and 1F). This high variability was not due to unreliable stimulation or measurement noise because response amplitudes were reproducible for repeated trials (trial-to-trial QCV: 0.12 ± 0.01, n = 12 cells, 3 trials per bouton, 1–5 boutons each). In dissociated culture, neighboring boutons show similar release parameters (Branco et al., 2008; Murthy et al., 1997; Peng et al., 2012) and RF scales with distance from the soma (Peng et al., 2012). We therefore tested SC boutons for local and global spatial correlations. RFs of directly neighboring boutons were not correlated (Figure 2A) (R^2 = 0.06 ± 0.04, n = 7 cells, not different from the correlation between random bouton pairs: R^2 = 0.01 ± 0.01, p = 0.46). Imaging conditions were near identical for adjacent boutons; we therefore could gain additional information by comparing absolute fluorescence signals of the

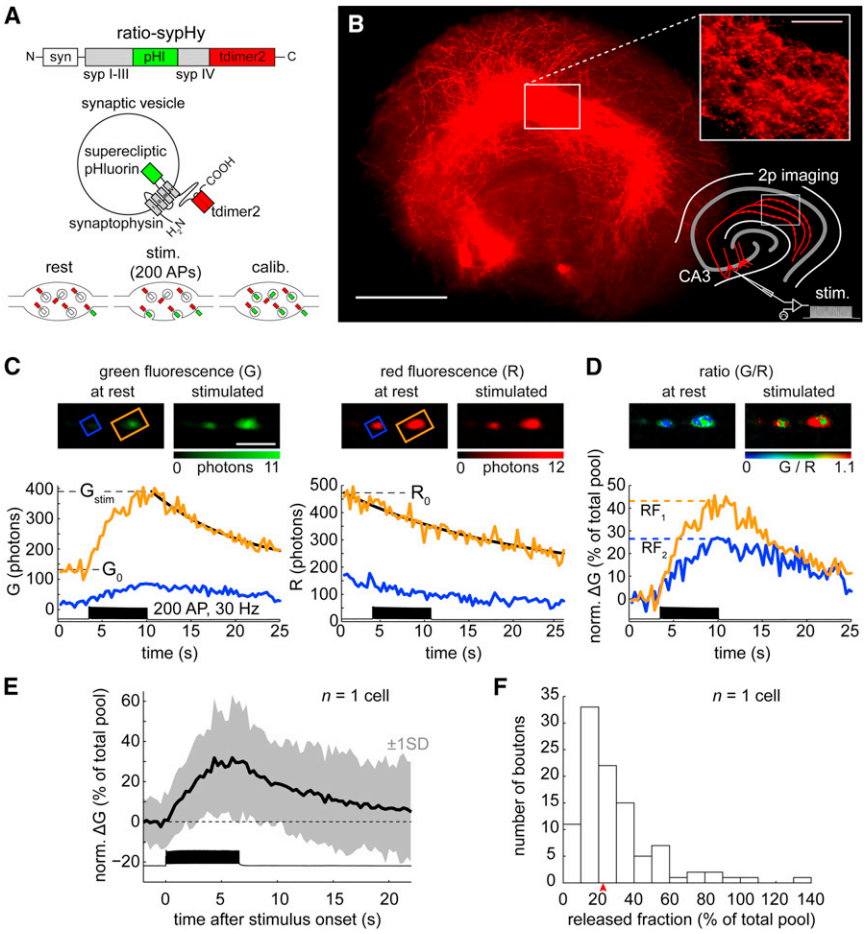

Figure 1. Assessment of Vesicle Cycle Parameters in Intact Tissue by Two-Photon Imaging of Ratio-sypHy

(A) Schematic representation of the ratio-sypHy-construct and measurement principle. Superecliptic pHluorin (pHl) is inserted between the third and fourth transmembrane domains of synaptophysin (syp) and faces the vesicular lumen. Dimeric RFP (tdimer2) is fused to the cytosolic carboxy-terminal. Lower panel: Strategy for ratiometric measurements. At rest, green fluorescence (G_0) is mainly due to surface-stranded protein (left). Stimulation-evoked exocytosis and exposure of vesicular pHluorin to the neutral extracellular pH leads to an increase in the fluorescence ratio ($\Delta G/R$) (middle). This can be expressed as the released fraction of vesicles by relating it to the calibration ratio (G_{max}/R) after NH_4Cl (right).

(B) Epifluorescence image of a hippocampal slice culture with three cells in CA3 expressing ratio-sypHy (scale bar: 500 μm). Insert: Punctate fluorescence in *stratum radiatum* (*s.r.*) of CA1 (scale bar: 100 μm).

(C) Ratio-sypHy reporting exo-/endocytosis. Green and red fluorescence of two mature Schaffer collateral (SC) boutons in response to an action potential (AP) train (200 APs, 30 Hz). Images are single optical sections (scale bar: 5 μm). Peak values (G_{stim}, R) were determined by fitting single exponential functions to the fluorescence decay (black curves).

(D) To determine the released fraction (RF) for each bouton, the G/R_0 ratio was normalized to the average G_{max}/R_0 (in NH_4Cl) at a different set of boutons and corrected for surface-stranded protein. See also Figure S1.

(E) RF at boutons along individual axons is heterogeneous. Average response of 101 vesicle clusters of a single CA3 pyramidal cell axon (± SD, gray area) during 200 APs at 30 Hz.

(F) Distribution of RFs (same data set as E). Note the broad range of observed RFs (quartile coefficient of variation, QCV: 0.42). Red arrow: population median (23% of total pool).

two-color channels independently. Total vesicle content (integrated red fluorescence, corrected for surface-stranded protein) and the absolute number of released vesicles (change of integrated green fluorescence) were also not correlated between neighbors (Figure 2B). None of the individual axons showed significant neighborhood correlations (data not shown). Furthermore, RF did not change as a function of distance along the axons (Figures 2C and 2D; average axon length studied: 338 ± 78 μm, range: 107–729 μm; n = 7 cells, 14–89 boutons each). Therefore, in contrast to dissociated culture (Branco et al., 2008; Murthy et al., 1997; Peng et al., 2012), mature SC boutons do not display systematic modulation of presynaptic parameters along the axon, locally or globally. Given that multiple synaptic connections between one axon and one dendritic branch are frequently formed in dissociated culture, but not in organotypic culture (Figure S2) or in vivo (Sorra and Harris, 1993), the lack of neighborhood correlations in organotypic culture is not surprising. SC axons traverse CA1 dendrites perpendicular (Figure S2), an arrangement that prevents retrograde comodulation of neighboring boutons by the same target cell (Branco et al., 2008).

Release Scales with Total Vesicle Number like Bouton Surface to Bouton Volume

Synaptic P_r scales linearly with the number of vesicles docked to the active zone (Branco et al., 2010; Holderith et al., 2012; Murthy et al., 2001). How release scales with the total vesicle number is less clear, given that not all vesicles are thought to be functional (Branco et al., 2010). Taking the integrated red fluorescence of ratio-sypHy as an estimate of total vesicle content (corrected for surface fraction), we were able to compare total vesicle pool size and RF at individual boutons along SC axons (Figure 3). We confirmed (Shepherd and Harris, 1998) that total vesicle content is highly variable (average QCV: 0.49 ± 0.02, n = 12 cells). The average RF in response to 200 APs at 30 Hz was nearly constant for the largest quartile ($Q_{75\%}$) of boutons (Figure 3B). The smallest quartile ($Q_{25\%}$), however, released on average an almost 2-fold larger fraction of their vesicles ($Q_{25\%}/Q_{75\%}$ = 1.8 ± 0.12, $p < 0.0001$, 74 boutons per quartile, n = 12 cells). Our data suggest that release scales with total vesicle content like bouton surface with bouton volume (i.e., 2/3 power; Figure 3B; also see the Experimental Procedures). Thus, during periods of high activity, small synapses are more prone to

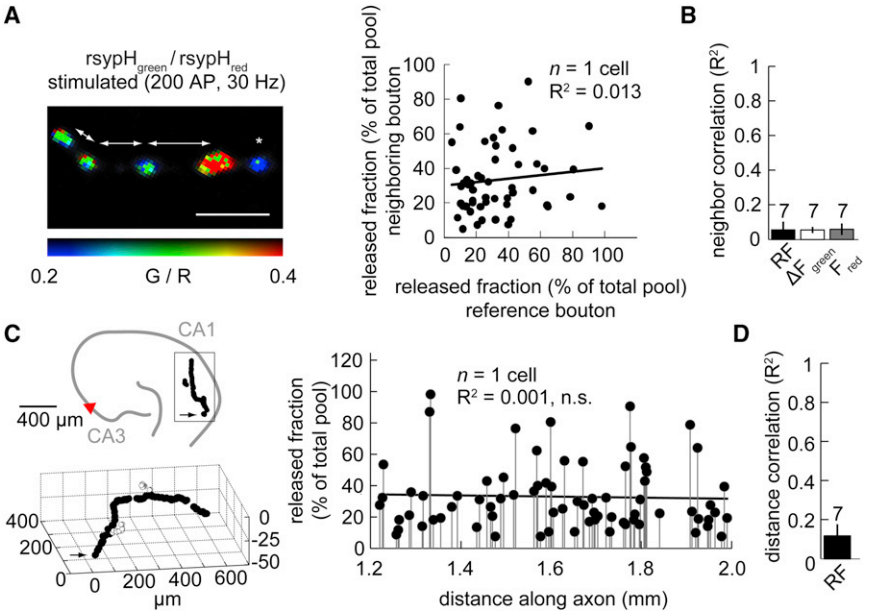

Figure 2. Release Properties along Schaffer Collaterals Are Not Correlated with Bouton Position

(A) Left: Ratio image of five SC boutons responding or not responding (asterisk) to stimulation with 200 APs at 30 Hz. Arrows indicate direct neighbors used for analysis of local relations. Right: RFs at neighboring boutons are not correlated (single axon).

(B) RF, presynaptic strength (increase in green fluorescence, ΔF_{green}), and vesicle cluster size (surface-corrected red fluorescence, F_{red}) were not correlated between neighboring boutons (n = 7 cells, 11–54 boutons each, separation range used: 1.5–10 µm).

(C) Spatial positions of functionally characterized boutons of a single SC axon (black circles) in relation to the stimulated cell body in CA3 (red triangle). RFs did not vary systematically with distance along the axon.

(D) No neuron (n = 7) showed a significant correlation between bouton position and RF. RFs were measured over an average axonal length of 338 ± 78 µm (range: 107–729 µm; 14–89 boutons/axon). Error bars represent SEM. See also Figure S2.

deplete their vesicles than large synapses. Part of the heterogeneity in RF (Figures 1E and 1F) can therefore be explained by differences in total vesicle content.

Functional Maturation of Schaffer Collateral Synapses

To investigate the functional maturation of SC synapses, we recorded responses from boutons in immature slice cultures (DIV 5–7). At this developmental stage, we frequently observed axonal growth cones in *stratum radiatum* (Figure 4A) but could already see clear AP-induced fluorescence transients in boutons. The decay of the fluorescence transient reflects the combined rates of endocytosis and subsequent vesicular reacidification (Atluri and Ryan, 2006; Granseth et al., 2006). In an attempt to separate these two steps, we fit our data with an established model that represents reacidification and endocytosis as two consecutive and irreversible first-order kinetic processes (Granseth et al., 2006). A good fit, however, was only possible under the assumption of rapid reacidification ($\tau \sim 0.5$ s; Figures S3C and S3D). Thus, under our conditions (25 mM $NaHCO_3$, 25°C), the speed of endocytosis limited the rate of fluorescence decay (Gandhi and Stevens, 2003). In the remainder of the study, to avoid overfitting, we used single exponential fits to estimate the time constant of endocytosis (τ). In immature SC boutons, we found $\tau = 39.0 \pm 8.5$ s (n = 6 cells; Figure 4B), more than threefold slower than in mature boutons ($\tau = 12.1 \pm 1.7$ s, n = 12 cells). In addition to the slow decay, peak amplitudes of the fluorescence ratio change triggered by 200 APs were small in immature slice culture. The median RF was only half as big as in mature boutons (16.6% ± 3.4% of the total pool, n = 8 cells, p = 0.02; Figure 4C). Together with the low rate of endocytosis, this corresponds to a 7-fold increase in the maximum vesicle retrieval rate approximated as RF/τ (retrieved SVs per second in percent of the total vesicle pool: mature slices RF/τ = 2.8%/s ± 0.4%/s versus immature slices RF/τ = 0.4%/s ± 0.1%/s, p = 0.0008).

To test the new indicator in a more established preparation, we also transfected dissociated hippocampal cultures with ratio-sypHy. Even after 2–4 weeks in the incubator, RFs were still significantly lower in this system (p = 0.003) (Figure 4C) and near identical to RFs in immature slice culture (p = 0.68). This corresponds well to the lower number of docked vesicles in dissociated culture (Schikorski and Stevens, 1997). Endocytic time constants were also significantly slower compared to mature synapses in tissue (p = 0.023) but not different from immature SC boutons (p = 0.16). The size-dependent scaling of RF that we observed in organtoypic culture (Figure 3) was not apparent in dissociated culture ($Q_{25\%}/Q_{75\%} = 1.3 \pm 0.18$, p = 0.30, 21 boutons per quartile, n = 5 cells). These findings suggest a prominent developmental refinement of vesicle cycle parameters at SC boutons that is not recapitulated in dissociated culture.

Developmental Elimination of Resting Vesicle Pool at Schaffer Collateral Boutons

To quantify the size of recycling and resting pools at SC synapses, we adapted the "alkaline trapping" method in which the vacuolar-type H^+-ATPase blocker bafilomycin A1 is applied to prevent vesicular reacidification after exocytosis (Burrone et al., 2006; Fernandez-Alfonso and Ryan, 2008; Fredj and Burrone, 2009; Li et al., 2005). The use of a ratiometric indicator enabled us to perform baseline measurements, tests of bafilomycin action, release measurements, and indicator calibration sequentially on different sets of boutons (Figure 5A). To ensure that bafilomycin had diffused into the tissue and taken effect, we repeatedly tested reacidifiaction on a set of "sentinel" boutons that were not used for pool quantification (Figure 5B). After successful block of reacidification, saturating stimulation (200 + 1,200 APs) ensured that all release-competent vesicles along the axon had been released at least once, resulting in an increased *G/R* fluorescence ratio (the "recycling ratio"). NH_4Cl was applied

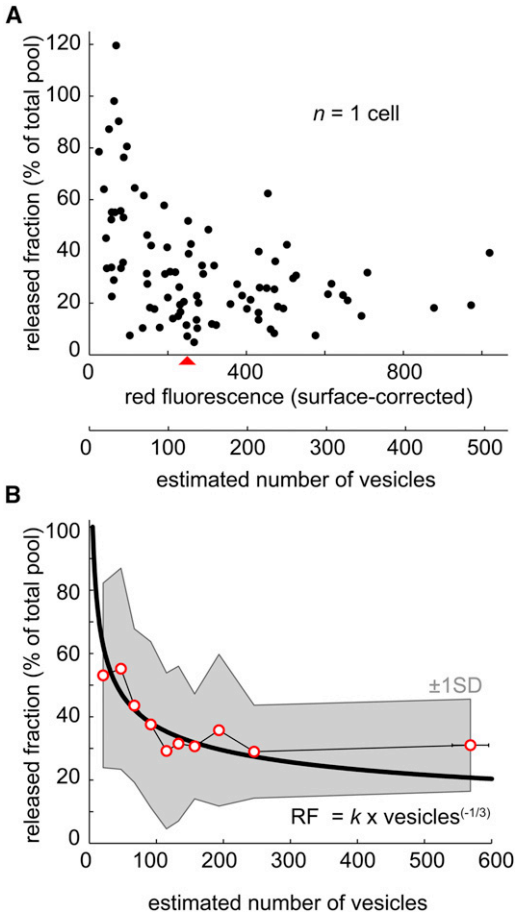

Figure 3. The Released Fraction Scales Nonlinearly with the Total Number of Vesicles at Schaffer Collateral Synapses

(A) Individual released fractions (boutons of a single cell) plotted against the integrated red intensity (surface expression-corrected) as a measure of vesicle cluster size at each bouton. To estimate the number of vesicles, the x axis was scaled to fit the median of the measured axonal distribution (red triangle) to the median number of synaptic vesicles at SC boutons (Shepherd and Harris, 1998).

(B) Pooled and binned (to ten percentiles) median-centered data of 297 boutons from 12 cells (red circles). Black curve: Fit of a surface-to-volume relationship between released vesicles and total number of vesicles (ves): RF = 172 × $ves^{-1/3}$.

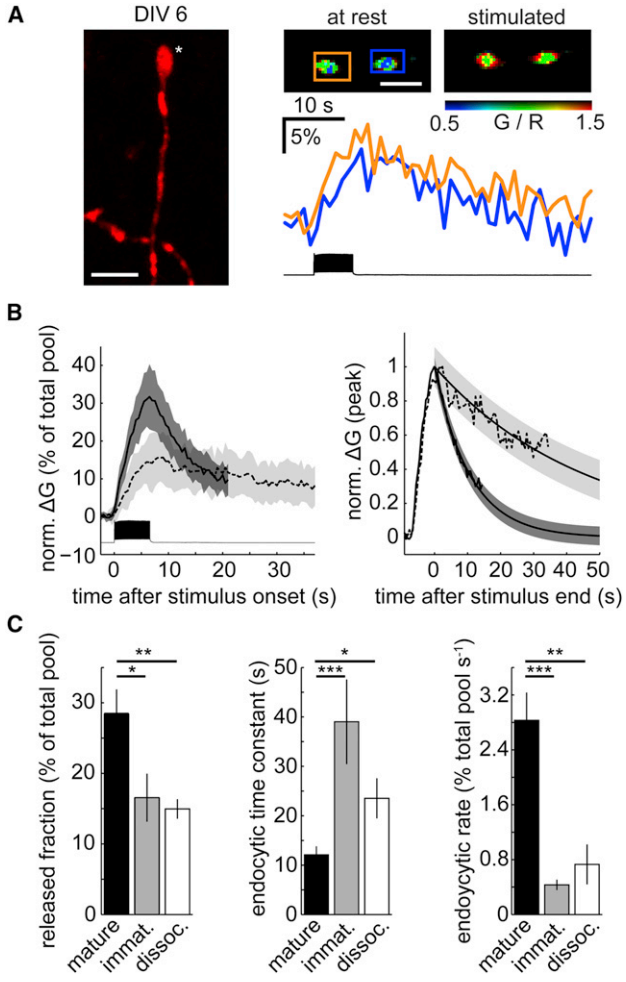

Figure 4. Developmental Increase in Released Fraction and Endocytic Speed at Schaffer Collateral Boutons

(A) Representative recording of two SC boutons in immature slice culture (DIV6). At this developmental stage, large growth cones were frequently visible in *stratum radiatum* (asterisk, scale bar 5 μm).

(B) Time course of normalized bouton fluorescence (mean of axonal average traces) in response to 200 APs in mature (DIV 14–28, n = 12 cells, solid line) and immature (DIV 5–7, n = 8 cells, dashed line) SC boutons. Right: Peak-normalized traces and single exponential fits through the fluorescence decay, showing differences in endocytic speed (τ mature: 11 s, 95% confidence interval, $CI_{95\%}$: 10.6–11.4 s versus τ immature: 46.2 s, $CI_{95\%}$: 43.8–48.9 s). Shaded areas indicate 95% confidence intervals.

(C) RF (average axonal median) and endocytic speed (average τ from fits through axonal average traces) in response to 200 APs at 30 Hz. Synapses in mature organotypic slices released 29% ± 3% of their total pool (n = 12 cells), whereas RFs were significantly reduced in immature slice cultures (RF = 17% ± 3%, n = 8 cells, p = 0.025) and in synapses between dissociated hippocampal neurons (RF = 15% ± 1%, n = 8 coverslips, p = 0.003). Endocytic time constants and endocytic rates (maximum retrieval rates, RF/τ) were fastest in mature organotypic slices (τ = 12 ± 1.7 s; RF/τ = 2.8% ± 0.4%/s), significantly slower in immature slice culture (τ = 39 ± 8.6 s, RF/τ = 0.4% ± 0.1%/s, n = 6 cells, p = 0.0006 and 0.0008) and in synapses between dissociated hippocampal neurons (τ = 24 ± 5.6 s; RF/τ = 1.5% ± 0.5%/s, n = 6 coverslips, p = 0.02 and 0.0026).

Bar graphs represent means ± SEM. In all figures, Student's t test (*p < 0.05, **p < 0.01, ***p < 0.001, n.s. p > 0.05) was used for statistical analysis. See also Figure S3.

at the end of the experiment to obtain the "calibration ratio" (G_{max}/R).

To our surprise, chemical alkalization did not further increase the average G/R ratio in mature SC boutons, indicating that electrical stimulation had triggered complete turnover of essentially *all* vesicles (Figure 5C). To validate our calibration approach, we employed an independent alkalization strategy using the protonophores nigericin (10 μM) and monensin (40 μM) in an external solution mimicking intracellular ion concentration and synaptic cleft pH (Fernandez-Alfonso and Ryan, 2008). Recycling pool sizes obtained in these experiments were not different from NH_4Cl calibration experiments (p = 0.84, data not shown). We therefore conclude that, within the limits of our technique,

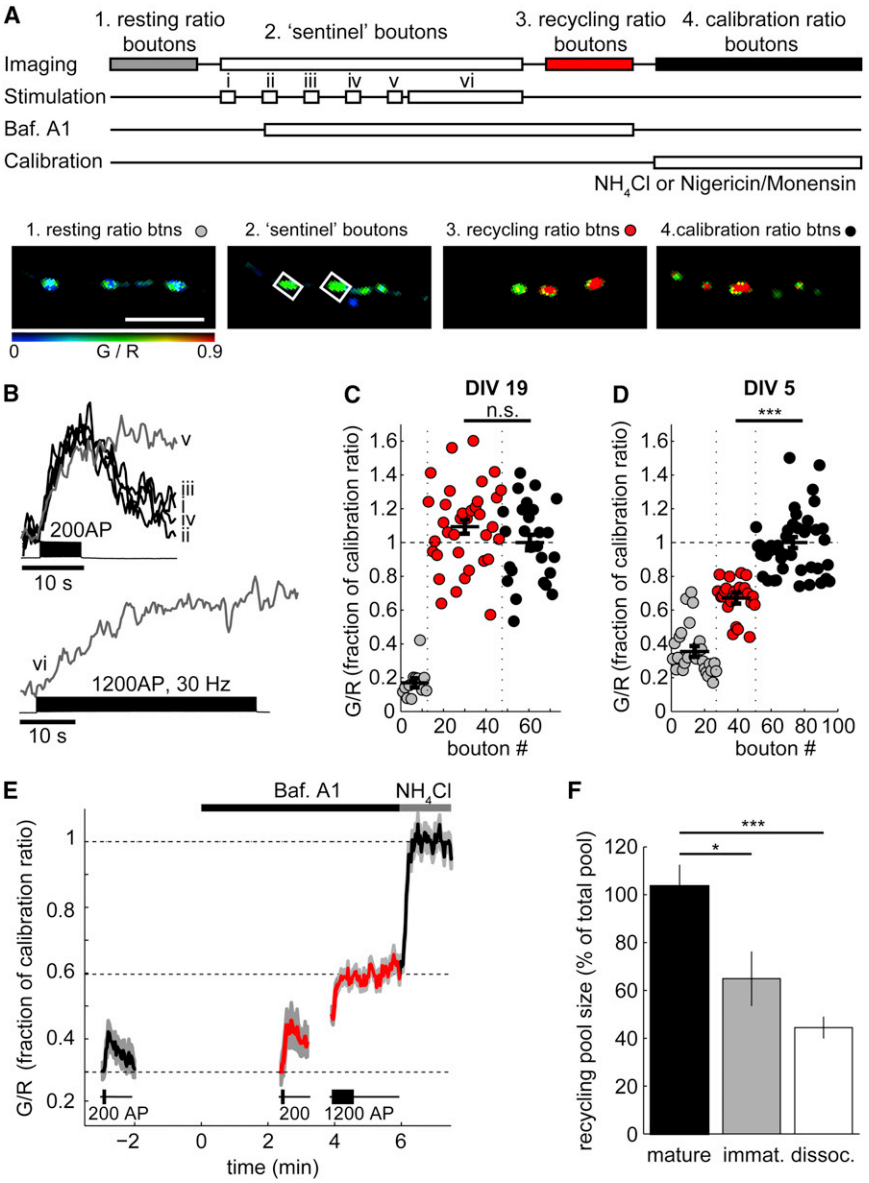

Figure 5. Mature Schaffer Collateral Boutons Mobilize Essentially All Vesicles during Saturating Stimulation

(A) Schematic representation of the alkaline trapping experiment. Following application of the vacuolar-type H^+-ATPase blocker bafilomycin A1 (Baf. A1, 2 μM), a small number of "sentinel" boutons was imaged during repetitive stimulation (200 APs, 30 Hz) to monitor the onset of drug action at the imaged axon (i to v). A saturating stimulus (1,200 APs, 30 Hz) was used to trap all releasable vesicles along the axon in the alkaline state (vi). To alkalize released and nonreleased vesicles alike, experiments were concluded by application of NH_4Cl or protonophores. Different sets of boutons were used for the four stages of the experiment (scale bar: 5 μm).

(B) Sentinel bouton responses (onset of bafilomycin action at trace v) and saturation of green fluorescence during 1,200 APs in bafilomycin (trace vi).

(C) Example of alkaline trapping experiment. The raw average recycling ratio (G_{rec}/R_0, red circles, coefficient of variation, CV 0.22) was not significantly different from the average calibration ratio (G_{max}/R_0, black circles, CV 0.23) after NH_4Cl application ($p = 0.17$), resulting in a recycling pool size of 108% of the total vesicle pool after correction for surface-stranded protein and spontaneous alkalization (see the Experimental Procedures).

(D) Example of alkaline trapping experiment in immature slice culture. Average recycling ratio and calibration ratio were significantly different ($p < 0.0001$, recycling pool size: 45%).

(E) Alkaline trapping in dissociated culture (recycling pool size: 38%).

(F) Summary of recycling pool estimates under different conditions (mature: 104% ± 9%, CV 0.35 ± 0.07, n = 8 cells; immature: 65% ± 11%, CV 0.45 ± 0.06, n = 7 cells; dissociated: 44% ± 5%, CV 0.54 ± 0.04, n = 7 coverslips).

Error bars represent SEM. See also Figures S4 and S5.

the recycling pool encompasses essentially all vesicles at mature SC boutons (104% ± 9%, n = 8 cells; Figure 5F). In a third set of experiments, we performed all steps of the alkaline trapping experiment on the same set of boutons. This strategy, which is standard for dissociated culture, is not optimal for slice culture because reliable measurements could only be obtained from a small number of closely spaced SC boutons (4–10 versus 13–50 boutons/cell). Again, the relative size of the recycling pool was close to maximal (89% ± 5%, n = 3 cells, p = 0.36) (Figure S4). In immature hippocampal slice cultures (DIV 5–7), we found a significantly smaller recycling pool (65% ± 11%, p = 0.018) (Figures 5D and 5F), indicating that the elimination of the resting pool is a developmental phenomenon. Synapses between dissociated hippocampal neurons had an even smaller recycling pool (45% ± 4%, p = 0.0009, Figures 5E and 5F) and recycling pool sizes of individual boutons were more variable (CV: 0.54 ± 0.04 versus 0.35 ± 0.07, p = 0.046). Differences in vesicle partitioning also explain why we found a size-dependence of the RF at SC synapses (Figure 3) but not at boutons in dissociated culture (see above). Here, any clear dependency between total vesicle number and RF is likely obscured by the large and highly variable resting pool size (Branco et al., 2010; Fernandez-Alfonso and Ryan, 2008; Harata et al., 2001; Ratnayaka et al., 2012).

Physiological Stimulation Confirms Large Recycling Pool at SC Boutons

It has been suggested that the intensity of the saturating stimulation protocol could affect recycling pool size (Denker and Rizzoli, 2010; Ikeda and Bekkers, 2009). Therefore, we wanted to assess whether the large recycling pool size is also evident during physiological levels of stimulation. To generate suitable

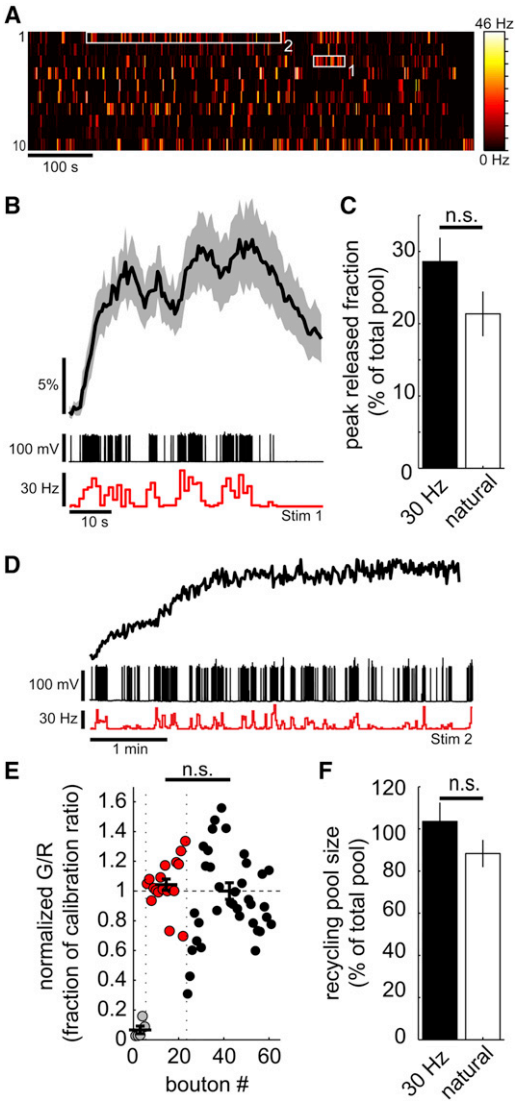

Figure 6. Physiological Stimulation Confirms Large Recycling Pool at SC Boutons

(A) Firing rate heatmaps (1 s bins) of ten CA3 cells recorded from a rat that was collecting randomly dispersed food in a rectangular enclosure. White boxes indicate activity patterns used for stimulation of CA3 cells in slice culture.

(B) Average time course of bouton fluorescence (in percent of total pool) in response to typical place field activity (n = 95 mature SC boutons, 13 cells). Gray shading indicates 95% confidence intervals. Middle panel: Representative current-clamp voltage trace (473 APs, average frequency 8.6 Hz). Lower panel: Instantaneous frequency (1 s bins).

(C) Peak RFs during place field activity (average axonal maximum, n = 13 cells) were comparable (p = 0.15) to peak RFs after 30 Hz stimulation (same data as in Figure 4C).

(D) Sentinel bouton response in bafilomycin, showing saturation of green fluorescence during natural spike train (1,370 APs).

(E) Alkaline trapping experiment using natural spike train. Calibration and recycling ratio were not different (p = 0.61). After correction for spontaneous alkalization (see the Experimental Procedures), recycling pool size was 105% in this example.

(F) The majority of vesicles was used during natural spike trains (88% ± 6.5%, CV 0.32 ± 0.07, n = 4 cells). In spite of lower average frequency (4.5 Hz), total vesicle use during natural spike train was not different from saturating stimulation at 30 Hz (p = 0.29).

Error bars represent SEM. See also Figure S5.

activity traces, we recorded from awake and moving rats using multiple tetrodes. Neuronal activity was recorded in CA3 while the rat was collecting randomly dispersed food in a rectangular enclosure with distinct visual cues on its walls. We selected ten neurons showing strong place preference. The resulting spike trains were played back as depolarizing current injections into CA3 cells in mature slice culture (Figure 6A; spike interval data available online as Supplemental Information). We found that during a 50 s stretch of place field activity, large fluorescence signals were induced. These signals correspond to the net balance of exocytosis and endocytosis and resemble a leaky integration of the instantaneous firing frequency (Figure 6B). During peaks of physiological activity, 22% of the total vesicle reserve accumulated at the synaptic surface, similar to the RF at the end of a 30 Hz 200 AP train (p = 0.15; Figure 6C). Do mature Schaffer collateral boutons eventually release and recycle all of their vesicles during natural activity? We performed alkaline trapping experiments using a 5 min stretch of replayed CA3 activity that contained 40 + 1,370 APs (Figure 6D), keeping the total number of APs similar to the 30 Hz train we used before to saturate vesicle turnover (Figure 5). Physiological stimulation mobilized 88% ± 6.5% of the total vesicle reserve (Figures 6E and 6F), not significantly different from our recycling pool measurements after high-frequency stimulation (p = 0.29). All alkaline trapping experiments were corrected for spontaneous alkalization (Figure S5).

Chronic Depolarization Induces Resting Pool Formation

Is it possible to induce resting pool formation at mature SC synapses? Chronic block of activity decreases resting pool size in dissociated culture (Kim and Ryan, 2010), whereas chronic depolarization completely silences a fraction of presynaptic boutons in autaptic preparations (Moulder et al., 2004). First, we tested whether CA3 cells are active under our culture conditions. Using on-cell recordings in culture medium at 35°C, we found similar average levels of spontaneous spiking activity in organotypic cultures of different age (immature cultures: 0.9 ± 0.3 Hz, n = 6 cells; mature: 0.9 ± 0.7 Hz, n = 11 cells; p = 0.98; data not shown). Thus, we could rule out absence of activity as a likely cause for the large recycling pool of mature SC synapses. To test the effects of chronic depolarization on pool partitioning, slice cultures were incubated overnight (16–18 hr) in culture medium containing 30 mM K^+. After this treatment, cells were allowed to recover for 45–60 min in standard extracellular solution. Alkaline trapping experiments revealed that chronic depolarization increased the number of unresponsive boutons (recycling fraction <1% of total pool) from 4% (9 out of 204 boutons) to 17% (24 out of 144 boutons). Furthermore, when we analyzed the responsive SC boutons, we found that a resting pool of ~35% was induced (Figure 7A). In response to our 200 AP test stimulus, chronically depolarized boutons released a significantly smaller fraction of their vesicles (Figure 7C). The total number of vesicles did not change after chronic depolarization (Figure S6), and the time constant of endocytosis

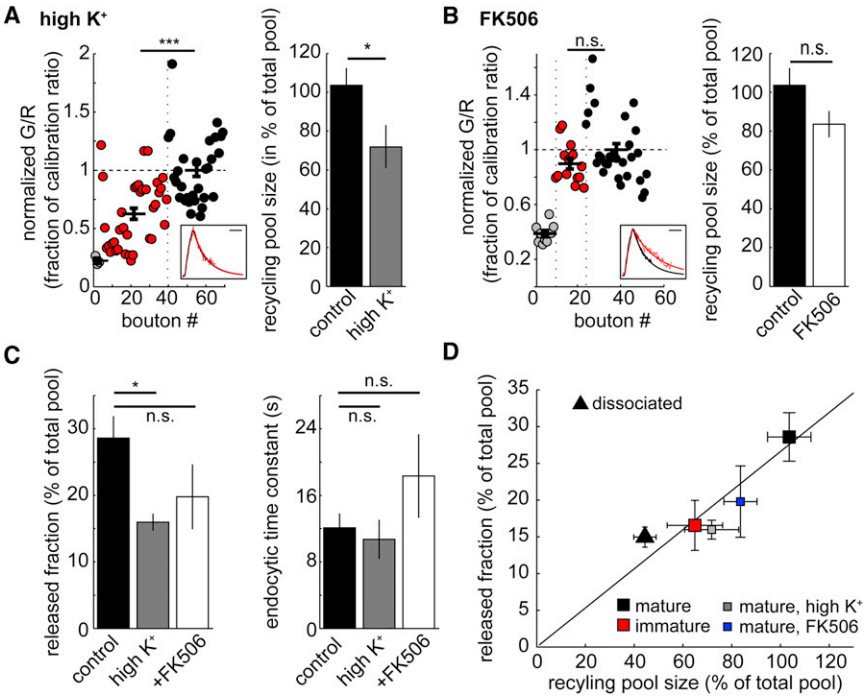

Figure 7. Effects of Chronic Depolarization and Calcineurin Inhibition on Recycling Pool Size and Endocytosis

(A) Example of alkaline trapping experiment following 16 hr incubation under depolarizing conditions (30 mM K^+). The average recycling ratio (red circles) was significantly smaller than the average calibration ratio (black circles) after NH_4Cl application ($p < 0.0001$), resulting in a recycling pool size of 40%. On average, prolonged depolarization led to a significant reduction of the recycling pool (72% ± 11%, CV 0.46 ± 0.1, n = 5 cells, p = 0.048). Endocytosis after 200 APs at 30 Hz was near identical to control (insert: average peak-normalized responses of control [black] and chronically depolarized [red] SC boutons).

(B) Under conditions of acute calcineurin block (1.5–2 hr of incubation in ACSF with 10 μM FK506), the raw average recycling ratio was not significantly different from the average calibration ratio in the example shown (p = 0.15, recycling pool size: 82%). On average, there was no evidence of a larger resting pool in the presence of FK506 (recycling pool size: 84% ± 6%, CV 0.39 ± 0.03, n = 6 cells, p = 0.12). Endocytosis was slowed down slightly in FK506 (insert: average peak-normalized responses of control [black] and FK506-treated [red] SC boutons).

(C) Chronically depolarized SC boutons released a smaller fraction of vesicles in response to 200 APs at 30 Hz (RF = 16% ± 2%, n = 5 cells, p = 0.019), whereas FK506 had no significant effect (RF = 20% ± 5%, n = 7 cells, p = 0.17). Endocytosis was unchanged after high K^+ incubation (τ = 10.7 ± 2.3 s, n = 3 cells, p = 0.46) and slightly slowed down by FK506 (τ = 18.3 ± 5.0 s, n = 6 cells, p = 0.16).

(D) Release during 200 APs scales with recycling pool size. Boutons released a fixed fraction of their recycling pool (linear fit: RF = 0.26 × recycling pool size; $R^2 = 0.81$) regardless of preparation (mature or immature slice culture [squares]; dissociated hippocampal culture [triangles]), activity-modulation paradigm (chronic depolarization [gray]), or pharmacological treatment (10 μM FK506 [blue]).

Error bars represent SEM. See also Figure S6.

was not affected (p = 0.37) (Figures 7A and 7C). Together, these experiments suggest that mature SC synapses respond to prolonged depolarization by removing vesicles from the recycling pool, thus gradually decreasing synaptic output. In a subset of synapses, this process leads to complete presynaptic silencing.

Effect of Acute Calcineurin Block on Pool Partitioning

Protein phosphorylation by cyclin-dependent kinase 5 (CDK5) and dephosphorylation by the calcium-dependent protein phosphatase calcineurin have been shown to regulate the balance between kinetically different modes of endocytosis (Evans and Cousin, 2007; Clayton et al., 2007; Sun et al., 2010) and to affect resting pool size (Kim and Ryan, 2010). At the calyx of Held, however, calcineurin loses its regulatory effect on endocytosis during maturation (Yamashita et al., 2010). We therefore tested whether pharmacological inhibition of calcineurin by the specific blocker FK506 would still affect vesicle cycling at mature SC boutons. Calcineurin block did not significantly decrease resting pool size after 1.5–2 hr of incubation (Figure 7B). The time constant of endocytosis was slightly slowed in FK506, but this effect was also not significant (Figure 7C). Vesicle retrieval rates were not significantly affected by FK506 (RF/τ = 1.5%/s ± 0.48%/s, p = 0.07, n = 8 cells). Because of cell-to-cell variability in average resting pool size (Fernandez-Alfonso and Ryan, 2008), we did not pool boutons from different axons but treated every axon as an independent experiment (n = #cells). Similar sized effects of FK506 with n = #boutons were found to be statistically significant (Marra et al., 2012).

Interestingly, across all preparations and pharmacological treatments, the amount of vesicles released during high-frequency AP trains scaled linearly with recycling pool size: in response to 200 APs, synapses on average released ~30% of their respective recycling pools (slope of the linear fit in Figure 7D). Thus, resting/recycling pool partitioning is likely to affect synaptic output, emphasizing the physiological relevance of the developmental regulation of recycling pool size. At mature synapses, however, drastic measures, such as chronic depolarization, have to be taken to induce a resting pool and thus decrease synaptic strength.

DISCUSSION

We found that SC boutons in hippocampal slice culture increase the efficiency of vesicle cycling during development by virtually eliminating the resting pool and profoundly accelerating endocytosis. Our finding that virtually all vesicles are release-competent is at odds with a recent study using photoconversion of FM1-43FX in acute hippocampal slices (Marra et al., 2012). With that method, a much smaller fraction of vesicles was found to be labeled (17%). When we assume that stimulation, dye

loading, and photoconversion were all saturating, the easiest way to reconcile our data with the FM dye results is to assume that the majority of release events at mature hippocampal synapses are very brief or require the formation of a small fusion pore (Aravanis et al., 2003; Harata et al., 2006; Klingauf et al., 1998; Richards et al., 2005; Zhang et al., 2009). Both would allow the release of H^+ and glutamate but would effectively prevent full FM1-43 staining of the vesicle membrane. Previous experiments have already suggested this to be the case (Harata et al., 2006; Zhang et al., 2009). Alternatively, could we have overestimated the recycling pool size by a factor of five? We consider an error of this magnitude unlikely, as we arrived at the same estimate using two calibration methods (NH_4Cl, Nigericin/Monensin), and developing a ratiometric indicator allowed us to use both the same (Figure S4) or, more importantly, different sets of boutons for measurement and calibration.

Developmental Changes of Endocytic Rate

We found a dramatic acceleration of vesicle cycling kinetics at developing SC synapses, similar to changes reported during maturation of the calyx of Held. In this giant synapse, containing hundreds of active zones (AZs) (Sätzler et al., 2002), the maximum vesicle retrieval rate at a given stimulation intensity increases dramatically after hearing onset (immature calyx: 0.2 SVs s^{-1} AZ^{-1}; mature calyx: 7.2 SVs s^{-1} AZ^{-1} [Renden and von Gersdorff, 2007]) and the readily releasable vesicle pool becomes twice as large (Taschenberger and von Gersdorff, 2000). If we assume an average of ~200 SV and a single AZ per SC bouton (Shepherd and Harris, 1998), our estimates of endocytosis from fluorescence decay measurements translate to retrieval rates of 0.9 SVs s^{-1} AZ^{-1} for immature and 5.7 SVs s^{-1} AZ^{-1} for mature boutons. It is striking that these synapses of very different size improve the performance of vesicle recycling during maturation in the same way, suggesting fundamental mechanisms that govern presynaptic development in intact tissue. Compared to mature synapses in tissue, retrieval rates that we (1.5 SVs s^{-1} AZ^{-1}) and others (1 SVs s^{-1} AZ^{-1} [Sankaranarayanan and Ryan, 2000]) measured in dissociated culture were markedly lower, even though these cultures had been kept in the incubator for several weeks. It had been noted previously that both endocytic rate and resting pool size in dissociated cells are stable between the second and third week in vitro (Armbruster and Ryan, 2011; Fernandez-Alfonso and Ryan, 2008), even though spine synapse formation in this preparation peaks at this time (Papa et al., 1995). This suggests that refinement of recycling capacity during development is typical for central synapses in tissue but does not proceed similarly in dissociated culture. It is tempting to speculate that the dramatically increased endocytic speed of mature SC boutons corresponds to a higher fraction of transient fusion events at mature synapses, potentially explaining the exceptionally low amount of dye-uptake observed by Marra et al. (2012).

Potential Links between Recycling Pathway and Resting Pool Size

The parallel developmental acceleration of endocytosis and virtual elimination of the resting pool at SC boutons raises the possibility that these events are coupled. It has been suggested that individual vesicles join the resting or the recycling pool depending on the recycling pathway chosen (Hua et al., 2011): resting pool vesicles are enriched with VAMP7 and vti1a, noncanonical endosomal SNARE proteins that are implicated in supporting spontaneous but not evoked neurotransmitter release (Hua et al., 2011; Ramirez et al., 2012). These findings indicate that resting and recycling vesicles participate in different modes of release and, potentially, undergo differential endosomal passage. The only identified molecular regulators of resting pool size, protein phosphorylation by CDK5 and dephosphorylation by calcineurin (Kim and Ryan, 2010), also determine the balance between conventional and bulk endocytic pathways in dissociated culture (Clayton et al., 2007; Evans and Cousin, 2007). Furthermore, CDK5 inhibition increases clathrin-mediated endocytic rates in the same preparation (Tomizawa et al., 2003). Conversely, calcineurin inhibition prominently slows down endocytosis at the immature calyx of Held and in dissociated hippocampal cultures (Sun et al., 2010). We find that at mature SC boutons, acute calcineurin block has only a slight inhibitory effect on endocytosis, much less pronounced than the up to 7-fold decrease in retrieval rate that has been reported for dissociated culture (Sun et al., 2010). Importantly, acute calcineurin block did not significantly change resting pool size at mature SC boutons, whereas calcineurin knockdown increases the resting pool in dissociated cells (Kim and Ryan, 2010). Together, this suggests that the effect of calcineurin on pool partitioning may lie downstream of its primary site of action, regulating endocytosis, and that calcineurin partially loses its regulatory role during maturation of hippocampal synapses, as has been shown for the calyx (Renden and von Gersdorff, 2007; Yamashita et al., 2010). A direct link between endocytic capacity and resting pool size is further supported by a recent study that showed a decreased recycling pool in mutant mouse-NMJs lacking cystein-string-protein-α that resulted in an inhibition of dynamin-mediated endocytosis (Rozas et al., 2012). The large resting pool we induced by overnight depolarization is also consistent with a causal role of endocytic pathways in resting pool formation: strong depolarization triggers modes of endocytosis that require extensive endosomal passage, for example, bulk endocytosis (Clayton et al., 2007), which seems to result in a large number of nonfunctional vesicles.

Physiological Relevance of Pool Partitioning

The essential lack of a resting pool at mature SC synapses has several important consequences. We and others (Murthy and Stevens, 1999) find that the amount of released vesicles during high-frequency stimulation scales directly with the recycling pool size, which, in turn, correlates with the probability of release in response to single APs (Murthy et al., 2001), potentially following simple laws of mass action. Changing the recycling fraction therefore emerged as an attractive concept of controlling presynaptic gain in lieu of bouton shrinkage or growth (Branco et al., 2010; Ratnayaka et al., 2012). Our data suggest that resting pool formation at mature small central synapses might take place under pathophysiological conditions, such as stroke or seizures, where high external K^+ concentrations are

known to occur in vivo (Moulder et al., 2004) and synaptic output has to be reduced to avoid excitotoxicity. Under physiological conditions, however, the recycling pool encompasses nearly all vesicles present in mature SC boutons. We conclude that at mature SC synapses, pool partitioning into resting and recycling pools does not play a major role for the activity-dependent regulation of synaptic strength.

Vesicle Use at Synapses In Vivo

We show that a sizeable fraction (more than 20%) of the available vesicles at SC boutons is released during typical place cell activity and that eventually the entire vesicle pool is turned over (Figure 6B). Using dye-uptake assays at neuromuscular junctions (NMJs) and other giant synapses, only a very small fraction of vesicles (1%–5%) has been reported to be used during actual behavior (Denker et al., 2011a). Clearly, small central synapses have evolved under a completely different set of constraints, sacrificing the absolute reliability of relay synapses like the calyx of Held or NMJs in order to maximize packaging density of the neuropil (Chklovskii et al., 2002; Varshney et al., 2006). A typical vertebrate motor neuron maintains less than 40 NMJs, whereas a CA3 pyramidal cell contacts about 40,000 postsynaptic neurons with minuscule synapses (Wittner et al., 2007). Both the signal-to-noise ratio of synaptic transmission and information storage capacity at such small synapses should benefit strongly from making the most efficient use of the available volume and vesicle resources (Varshney et al., 2006). Consistent with these theoretical considerations, we find an inverse correlation between the total number of vesicles present in a bouton and the fraction that is released during a test stimulus (Figure 3). Interestingly, if we extend this surface-to-volume relationship to the size of a mouse calyx that contains ~200,000 SVs and has an approximately 5-fold lower ratio of combined AZ surface area to synapse volume (Sätzler et al., 2002; Schikorski and Stevens, 1997), we arrive at a released fraction of 3%. Similar values have been reported by Denker and colleagues after strong stimulation in vivo. Thus, we see no contradiction in the fact that we find a high released fraction during physiological stimulation of very small synapses while giant relay synapses apparently use only a few percent of their total vesicle reserve. Our finding that mature SC boutons have a much larger proportion of active vesicles than previously thought at least partially resolves the conundrum how fast neurotransmission can be sustained at these miniaturized synapses (Harata et al., 2001). By combining a large number of functional vesicles with efficient endocytosis, mature SC synapses appear well equipped to sustain transmission during high-frequency place cell firing in vivo.

EXPERIMENTAL PROCEDURES

Methods are described in greater detail in the Supplemental Experimental Procedures.

Preparation and Transfection of Hippocampal Cultures

Organotypic hippocampal slice cultures were prepared from Wistar rats at p5 and either transfected at DIV 1–2 and imaged at DIV 5–7 ("immature") or transfected at DIV 5–6 and imaged 1–3 weeks later, typically DIV 20 ("mature"). Dissociated rat hippocampal cultures were transfected by electroporation (Nucleofector, Amaxa) and imaged between DIV 17 and 26 (typically DIV 20).

Electrophysiology

Slice cultures were superfused with artificial cerebrospinal fluid (ACSF) containing (in mM) 127 NaCl, 2.5 KCl, 2 $CaCl_2$, 1 $MgCl_2$, 25 $NaHCO_3$, 1.25 NaH_2PO_4, 25 D-glucose, 0.01 NBQX, and 0.01 R-CPP, gassed with 95% O_2 and 5% CO_2 (pH 7.4). Recording pipettes (4–7 MΩ) were filled with intracellular solution containing (in mM) 135 K-gluconate, 10 HEPES, 4 $MgCl_2$, 4 Na_2-ATP, 0.4 Na_2-GTP, 10 Na_2-phosphocreatine, 3 ascorbate, and 0.3 EGTA (pH 7.3). Dissociated hippocampal cells were constantly superfused with a solution containing (in mM) 136 NaCl, 2.5 KCl, 10 mM HEPES, 10 mM D-glucose, 2 $CaCl_2$, 1 $MgCl_2$, 0.01 NBQX, and 0.01 R-CPP (pH 7.4). To stimulate dissociated cultures, brief current pulses (1 ms, 10–30 mA) were applied to two parallel platinum wires using a stimulus isolator (WPI A385). Current amplitude was adjusted to maximize the change in ratio-sypHy fluorescence in response to trains of 40 APs at 30 Hz. All experiments were performed at 25°C ± 1°C by controlling the temperature of the perfusate and the oil immersion condenser (HeatWave-30, Dagan, Minneapolis, MN, USA).

Two-Photon Imaging

We used a custom-built two-photon microscope based on a BX51WI microscope (Olympus, Center Valley, PA, USA) and the open source software ScanImage (Pologruto et al., 2003). A Ti:Sapph laser (Chameleon XR, Coherent, Santa Clara, CA, USA) was tuned to λ = 930 nm to excite red and green fluorescence of ratio-sypHy. Fluorescence was detected through the objective (LUMPlan W-IR2 60×, 0.9 NA, Olympus) and through the oil immersion condenser (1.4 NA, Olympus) using photomultiplier tubes (R3896, H7422P-40, Hamamatsu, Bridgewater, NJ, USA) and band pass filters (525/50, 610/75, Chroma). Frame rates were 3.3 Hz (slice culture) and 2 Hz (dissociated culture).

Data Analysis

We used the red fluorescence signal to automatically detect individual boutons (Matlab). Images were background-subtracted and corrected for optical crosstalk. G_0 was determined by averaging the ROI intensities of the green channel over the first 5–9 frames preceding stimulation. We determined the average bleach rate per axon by performing a monoexponential fit over the average fluorescence time course of unresponsive boutons. Bleach rates on the green channel were similar for all conditions, including dissociated cells (τ = 4.2 ± 0.3 min; n = 30 cells, eight dishes; p = 0.44, ANOVA), and data from all cells were corrected accordingly (Figures S1A and S1B). A single exponential fit to the decay phase (starting 500 ms after the end of stimulation) was used to define the time constant for endocytosis (τ) and G_{stim} ($G_{(t)}$ = $G_{stim} \times e^{\wedge}(-t_{stim+500ms}/\tau)$). R was defined as the first point of a single exponential fit through the entire red fluorescence time course (also see Figures S3C and S3D).

Ratiometric Calculation of Released and Recycling Fractions

To determine the released fraction (RF) for each bouton, the G/R_0 ratio was normalized to the average G_{max}/R_0 (in NH_4Cl) at a different set of boutons and corrected for surface-stranded protein.

By comparing the effective dynamic range of ratio-sypHy,

$$\gamma = \frac{G_{max}/R_0 - G_0/R}{G_0/R}, \qquad \text{(Equation 1)}$$

(γ = 3.17, n = 922 boutons) with the dynamic range of superecliptic pHluorin for the same pH change (α = 20.7; Sankaranarayanan et al., 2000), we could estimate the fraction of surface-stranded ratio-sypHy (f_{surf}) (Sankaranarayanan et al., 2000),

$$f_{surf} = \frac{\alpha - \gamma}{\alpha\gamma + \alpha}. \qquad \text{(Equation 2)}$$

To correct the evoked ratio changes for surface-stranded indicator molecules, we calculated f_{surf} for each bouton, which allowed us to derive

the vesicular red fluorescence (R_{ves} = ($1-f_{surf}$) × R) for every synapse. Assuming equal distribution of ratio-sypHy over all vesicles (Fernandez-Alfonso and Ryan, 2008), we approximated the "released fraction" (*RF*), the number of vesicles released in response to the stimulus divided by the total number of vesicles present at the synapse (in percent), as

$$RF = \frac{\Delta G/R_{ves}}{G_{max}/R} \times 100. \quad \text{(Equation 3)}$$

We assessed the uncorrected (see below) recycling pool size (*RecF*) as

$$RecF = \frac{G_{rec}/R - G_0/R}{G_{max}/R - G_0/R} \times 100. \quad \text{(Equation 4)}$$

G_{rec}/R represents the individual fluorescence ratios of boutons whose recycling vesicles were trapped in an alkaline state after bafilomycin A1 application and subsequent saturating stimulation (1,400 APs). G_0/R is the average resting ratio of a different set of boutons before stimulation, and G_{max}/R is the average calibration ratio of a further set of boutons. We estimate the rate of spontaneous increase in baseline pHluorin fluorescence after bafilomycin A1 application by fitting a monoexponential function through the normalized fluorescence increase ($100 \times G/G_{max}$) in the absence of stimulation (Figure S5):

$$F(t) = 100 - e^{\wedge}\left(\frac{-t}{\tau}\right) \quad \text{(Equation 5)}$$

(τ = 58 min, n = 3 slices). The duration of a natural stimulation experiment could reach up to 15 min; therefore, we needed to correct the recycling pool estimates of every bouton for this factor (Figure S5):

$$RecF_{corr} = 100 \times \frac{F(t) - RecF}{F(t) - 100}. \quad \text{(Equation 6)}$$

All released and recycling fractions are expressed as percent of the total vesicle pool.

Derivation of Size-Dependent Release Scaling

Anatomically, the total number of vesicles at a synapse is correlated with bouton volume (Knott et al., 2006; Murthy et al., 2001). Vesicular release, on the other hand, is restricted to the active zone at the surface of the bouton. Linear scaling has been demonstrated between P_r and the number of surface-docked vesicles (Murthy et al., 2001). Therefore, the most straightforward assumption would be linear scaling between the number of released vesicles (R) and bouton surface area (A): $R = k \times A$ (with k being a proportionality factor), equivalent to a 2/3-power scaling with bouton volume (V): $R = k \times V^{2/3}$. If all vesicles were functional, V could be substituted with the total number of vesicles (ves) filling the volume of the bouton. In this case, RF would be expected to scale as $RF = k \times ves^{-1/3}$. As shown in Figure 3B (black curve), this surface-to-volume function fits our data well ($RF = 172 \times ves^{-1/3}$).

Statistical Analysis

Data are reported as mean ± SEM unless indicated otherwise. To test for significance between population means, we used the two-tailed Student's t test. As nonparametric measures of absolute and relative dispersion of single bouton data, we use the interquartile range (IQR): $Q_{75\%} - Q_{25\%}$ and the quartile coefficient of variation (QCV): $(Q_{75\%} - Q_{25\%}) / (Q_{75\%} + Q_{25\%})$, respectively. All correlations are expressed as squared Pearson's correlation coefficients (R^2). Statistical significance was assumed when $p < 0.05$. Boundaries used for assigning significance in figures: not significant (n.s.), $p > 0.05$; significant, $p < 0.05$ (*), $p < 0.01$ (**), and $p < 0.001$ (***).

SUPPLEMENTAL INFORMATION

Supplemental Information includes six figures and Supplemental Experimental Procedures and can be found with this article online at http://dx.doi.org/10.1016/j.neuron.2013.01.021.

ACKNOWLEDGMENTS

This work was supported by the Novartis Research Foundation, SystemsX.ch, and the Kavli Foundation. The authors thank Daniela Gerosa for excellent technical assistance; Yongling Zhu and Charles F. Stevens for the gift of sypHluorin-1X; Roger Y. Tsien for tdimer2; and Corette Wierenga, Volker Scheuss, and the members of the Oertner lab for critically reading the manuscript.

Accepted: January 18, 2013
Published: March 20, 2013

REFERENCES

Aravanis, A.M., Pyle, J.L., and Tsien, R.W. (2003). Single synaptic vesicles fusing transiently and successively without loss of identity. Nature *423*, 643–647.

Armbruster, M., and Ryan, T.A. (2011). Synaptic vesicle retrieval time is a cell-wide rather than individual-synapse property. Nat. Neurosci. *14*, 824–826.

Atluri, P.P., and Ryan, T.A. (2006). The kinetics of synaptic vesicle reacidification at hippocampal nerve terminals. J. Neurosci. *26*, 2313–2320.

Bolshakov, V.Y., and Siegelbaum, S.A. (1995). Regulation of hippocampal transmitter release during development and long-term potentiation. Science *269*, 1730–1734.

Borst, J.G., and Soria van Hoeve, J. (2012). The calyx of held synapse: from model synapse to auditory relay. Annu. Rev. Physiol. *74*, 199–224.

Branco, T., Staras, K., Darcy, K.J., and Goda, Y. (2008). Local dendritic activity sets release probability at hippocampal synapses. Neuron *59*, 475–485.

Branco, T., Marra, V., and Staras, K. (2010). Examining size-strength relationships at hippocampal synapses using an ultrastructural measurement of synaptic release probability. J. Struct. Biol. *172*, 203–210.

Burrone, J., Li, Z., and Murthy, V.N. (2006). Studying vesicle cycling in presynaptic terminals using the genetically encoded probe synaptopHluorin. Nat. Protoc. *1*, 2970–2978.

Chklovskii, D.B., Schikorski, T., and Stevens, C.F. (2002). Wiring optimization in cortical circuits. Neuron *34*, 341–347.

Clayton, E.L., Evans, G.J., and Cousin, M.A. (2007). Activity-dependent control of bulk endocytosis by protein dephosphorylation in central nerve terminals. J. Physiol. *585*, 687–691.

de Lange, R.P., de Roos, A.D., and Borst, J.G. (2003). Two modes of vesicle recycling in the rat calyx of Held. J. Neurosci. *23*, 10164–10173.

De Simoni, A., Griesinger, C.B., and Edwards, F.A. (2003). Development of rat CA1 neurones in acute versus organotypic slices: role of experience in synaptic morphology and activity. J. Physiol. *550*, 135–147.

Denker, A., and Rizzoli, S.O. (2010). Synaptic vesicle pools: an update. Front. Synaptic Neurosci. *2*, 135.

Denker, A., Bethani, I., Kröhnert, K., Körber, C., Horstmann, H., Wilhelm, B.G., Barysch, S.V., Kuner, T., Neher, E., and Rizzoli, S.O. (2011a). A small pool of vesicles maintains synaptic activity in vivo. Proc. Natl. Acad. Sci. USA *108*, 17177–17182.

Denker, A., Kröhnert, K., Bückers, J., Neher, E., and Rizzoli, S.O. (2011b). The reserve pool of synaptic vesicles acts as a buffer for proteins involved in synaptic vesicle recycling. Proc. Natl. Acad. Sci. USA *108*, 17183–17188.

Evans, G.J., and Cousin, M.A. (2007). Activity-dependent control of slow synaptic vesicle endocytosis by cyclin-dependent kinase 5. J. Neurosci. *27*, 401–411.

Feldmeyer, D., and Radnikow, G. (2009). Developmental alterations in the functional properties of excitatory neocortical synapses. J. Physiol. *587*, 1889–1896.

Fernandez-Alfonso, T., and Ryan, T.A. (2008). A heterogeneous "resting" pool of synaptic vesicles that is dynamically interchanged across boutons in mammalian CNS synapses. Brain Cell Biol. *36*, 87–100.

Fredj, N.B., and Burrone, J. (2009). A resting pool of vesicles is responsible for spontaneous vesicle fusion at the synapse. Nat. Neurosci. *12*, 751–758.

Gandhi, S.P., and Stevens, C.F. (2003). Three modes of synaptic vesicular recycling revealed by single-vesicle imaging. Nature *423*, 607–613.

Granseth, B., Odermatt, B., Royle, S.J., and Lagnado, L. (2006). Clathrin-mediated endocytosis is the dominant mechanism of vesicle retrieval at hippocampal synapses. Neuron *51*, 773–786.

Harata, N., Ryan, T.A., Smith, S.J., Buchanan, J., and Tsien, R.W. (2001). Visualizing recycling synaptic vesicles in hippocampal neurons by FM 1-43 photoconversion. Proc. Natl. Acad. Sci. USA *98*, 12748–12753.

Harata, N.C., Choi, S., Pyle, J.L., Aravanis, A.M., and Tsien, R.W. (2006). Frequency-dependent kinetics and prevalence of kiss-and-run and reuse at hippocampal synapses studied with novel quenching methods. Neuron *49*, 243–256.

Holderith, N., Lorincz, A., Katona, G., Rózsa, B., Kulik, A., Watanabe, M., and Nusser, Z. (2012). Release probability of hippocampal glutamatergic terminals scales with the size of the active zone. Nat. Neurosci. *15*, 988–997.

Hua, Z., Leal-Ortiz, S., Foss, S.M., Waites, C.L., Garner, C.C., Voglmaier, S.M., and Edwards, R.H. (2011). v-SNARE composition distinguishes synaptic vesicle pools. Neuron *71*, 474–487.

Ikeda, K., and Bekkers, J.M. (2009). Counting the number of releasable synaptic vesicles in a presynaptic terminal. Proc. Natl. Acad. Sci. USA *106*, 2945–2950.

Kim, S.H., and Ryan, T.A. (2010). CDK5 serves as a major control point in neurotransmitter release. Neuron *67*, 797–809.

Klingauf, J., Kavalali, E.T., and Tsien, R.W. (1998). Kinetics and regulation of fast endocytosis at hippocampal synapses. Nature *394*, 581–585.

Knott, G.W., Holtmaat, A., Wilbrecht, L., Welker, E., and Svoboda, K. (2006). Spine growth precedes synapse formation in the adult neocortex in vivo. Nat. Neurosci. *9*, 1117–1124.

Li, Z., Burrone, J., Tyler, W.J., Hartman, K.N., Albeanu, D.F., and Murthy, V.N. (2005). Synaptic vesicle recycling studied in transgenic mice expressing synaptopHluorin. Proc. Natl. Acad. Sci. USA *102*, 6131–6136.

Lorteije, J.A., Rusu, S.I., Kushmerick, C., and Borst, J.G. (2009). Reliability and precision of the mouse calyx of Held synapse. J. Neurosci. *29*, 13770–13784.

Marra, V., Burden, J.J., Thorpe, J.R., Smith, I.T., Smith, S.L., Häusser, M., Branco, T., and Staras, K. (2012). A preferentially segregated recycling vesicle pool of limited size supports neurotransmission in native central synapses. Neuron *76*, 579–589.

Miesenböck, G., De Angelis, D.A., and Rothman, J.E. (1998). Visualizing secretion and synaptic transmission with pH-sensitive green fluorescent proteins. Nature *394*, 192–195.

Moulder, K.L., Meeks, J.P., Shute, A.A., Hamilton, C.K., de Erausquin, G., and Mennerick, S. (2004). Plastic elimination of functional glutamate release sites by depolarization. Neuron *42*, 423–435.

Mozhayeva, M.G., Sara, Y., Liu, X., and Kavalali, E.T. (2002). Development of vesicle pools during maturation of hippocampal synapses. J. Neurosci. *22*, 654–665.

Murthy, V.N., and Stevens, C.F. (1999). Reversal of synaptic vesicle docking at central synapses. Nat. Neurosci. *2*, 503–507.

Murthy, V.N., Sejnowski, T.J., and Stevens, C.F. (1997). Heterogeneous release properties of visualized individual hippocampal synapses. Neuron *18*, 599–612.

Murthy, V.N., Schikorski, T., Stevens, C.F., and Zhu, Y. (2001). Inactivity produces increases in neurotransmitter release and synapse size. Neuron *32*, 673–682.

Papa, M., Bundman, M.C., Greenberger, V., and Segal, M. (1995). Morphological analysis of dendritic spine development in primary cultures of hippocampal neurons. J. Neurosci. *15*, 1–11.

Peng, X., Parsons, T.D., and Balice-Gordon, R.J. (2012). Determinants of synaptic strength vary across an axon arbor. J. Neurophysiol. *107*, 2430–2441.

Pologruto, T.A., Sabatini, B.L., and Svoboda, K. (2003). ScanImage: flexible software for operating laser scanning microscopes. Biomed. Eng. Online *2*, 13.

Ramirez, D.M., Khvotchev, M., Trauterman, B., and Kavalali, E.T. (2012). Vti1a identifies a vesicle pool that preferentially recycles at rest and maintains spontaneous neurotransmission. Neuron *73*, 121–134.

Ratnayaka, A., Marra, V., Bush, D., Burden, J.J., Branco, T., and Staras, K. (2012). Recruitment of resting vesicles into recycling pools supports NMDA receptor-dependent synaptic potentiation in cultured hippocampal neurons. J. Physiol. *590*, 1585–1597.

Renden, R., and von Gersdorff, H. (2007). Synaptic vesicle endocytosis at a CNS nerve terminal: faster kinetics at physiological temperatures and increased endocytotic capacity during maturation. J. Neurophysiol. *98*, 3349–3359.

Reyes, A., and Sakmann, B. (1999). Developmental switch in the short-term modification of unitary EPSPs evoked in layer 2/3 and layer 5 pyramidal neurons of rat neocortex. J. Neurosci. *19*, 3827–3835.

Richards, D.A., Bai, J., and Chapman, E.R. (2005). Two modes of exocytosis at hippocampal synapses revealed by rate of FM1-43 efflux from individual vesicles. J. Cell Biol. *168*, 929–939.

Rizzoli, S.O., and Betz, W.J. (2005). Synaptic vesicle pools. Nat. Rev. Neurosci. *6*, 57–69.

Rozas, J.L., Gómez-Sánchez, L., Mircheski, J., Linares-Clemente, P., Nieto-González, J.L., Vázquez, M.E., Luján, R., and Fernández-Chacón, R. (2012). Motorneurons require cysteine string protein-α to maintain the readily releasable vesicular pool and synaptic vesicle recycling. Neuron *74*, 151–165.

Sankaranarayanan, S., and Ryan, T.A. (2000). Real-time measurements of vesicle-SNARE recycling in synapses of the central nervous system. Nat. Cell Biol. *2*, 197–204.

Sankaranarayanan, S., De Angelis, D., Rothman, J.E., and Ryan, T.A. (2000). The use of pHluorins for optical measurements of presynaptic activity. Biophys. J. *79*, 2199–2208.

Sätzler, K., Söhl, L.F., Bollmann, J.H., Borst, J.G., Frotscher, M., Sakmann, B., and Lübke, J.H. (2002). Three-dimensional reconstruction of a calyx of Held and its postsynaptic principal neuron in the medial nucleus of the trapezoid body. J. Neurosci. *22*, 10567–10579.

Schikorski, T., and Stevens, C.F. (1997). Quantitative ultrastructural analysis of hippocampal excitatory synapses. J. Neurosci. *17*, 5858–5867.

Schikorski, T., and Stevens, C.F. (2001). Morphological correlates of functionally defined synaptic vesicle populations. Nat. Neurosci. *4*, 391–395.

Shepherd, G.M., and Harris, K.M. (1998). Three-dimensional structure and composition of CA3—>CA1 axons in rat hippocampal slices: implications for presynaptic connectivity and compartmentalization. J. Neurosci. *18*, 8300–8310.

Sonntag, M., Englitz, B., Typlt, M., and Rübsamen, R. (2011). The calyx of held develops adult-like dynamics and reliability by hearing onset in the mouse in vivo. J. Neurosci. *31*, 6699–6709.

Sorra, K.E., and Harris, K.M. (1993). Occurrence and three-dimensional structure of multiple synapses between individual radiatum axons and their target pyramidal cells in hippocampal area CA1. J. Neurosci. *13*, 3736–3748.

Sun, T., Wu, X.S., Xu, J., McNeil, B.D., Pang, Z.P., Yang, W., Bai, L., Qadri, S., Molkentin, J.D., Yue, D.T., and Wu, L.G. (2010). The role of calcium/calmodulin-activated calcineurin in rapid and slow endocytosis at central synapses. J. Neurosci. *30*, 11838–11847.

Taschenberger, H., and von Gersdorff, H. (2000). Fine-tuning an auditory synapse for speed and fidelity: developmental changes in presynaptic waveform, EPSC kinetics, and synaptic plasticity. J. Neurosci. *20*, 9162–9173.

Tomizawa, K., Sunada, S., Lu, Y.F., Oda, Y., Kinuta, M., Ohshima, T., Saito, T., Wei, F.Y., Matsushita, M., Li, S.T., et al. (2003). Cophosphorylation of amphiphysin I and dynamin I by Cdk5 regulates clathrin-mediated endocytosis of synaptic vesicles. J. Cell Biol. *163*, 813–824.

Varshney, L.R., Sjöström, P.J., and Chklovskii, D.B. (2006). Optimal information storage in noisy synapses under resource constraints. Neuron *52*, 409–423.

Wittner, L., Henze, D.A., Záborszky, L., and Buzsáki, G. (2007). Three-dimensional reconstruction of the axon arbor of a CA3 pyramidal cell recorded and filled in vivo. Brain Struct. Funct. *212*, 75–83.

Wu, X.S., McNeil, B.D., Xu, J., Fan, J., Xue, L., Melicoff, E., Adachi, R., Bai, L., and Wu, L.G. (2009). Ca(2+) and calmodulin initiate all forms of endocytosis during depolarization at a nerve terminal. Nat. Neurosci. *12*, 1003–1010.

Yamashita, T., Eguchi, K., Saitoh, N., von Gersdorff, H., and Takahashi, T. (2010). Developmental shift to a mechanism of synaptic vesicle endocytosis requiring nanodomain Ca2+. Nat. Neurosci. *13*, 838–844.

Zhang, Q., Li, Y., and Tsien, R.W. (2009). The dynamic control of kiss-and-run and vesicular reuse probed with single nanoparticles. Science *323*, 1448–1453.